nature nanotechnology

LETTERS

PUBLISHED ONLINE: 16 NOVEMBER 2015 | DOI: 10.1038/NNANO.2015.260

A flexoelectric microelectromechanical system on silicon

Umesh Kumar Bhaskar[1*†], Nirupam Banerjee[2†], Amir Abdollahi[1], Zhe Wang[3], Darrell G. Schlom[3,4], Guus Rijnders[2] and Gustau Catalan[1,5*]

Flexoelectricity allows a dielectric material to polarize in response to a mechanical bending moment[1] and, conversely, to bend in response to an electric field[2]. Compared with piezoelectricity, flexoelectricity is a weak effect of little practical significance in bulk materials. However, the roles can be reversed at the nanoscale[3]. Here, we demonstrate that flexoelectricity is a viable route to lead-free microelectromechanical and nanoelectromechanical systems. Specifically, we have fabricated a silicon-compatible thin-film cantilever actuator with a single flexoelectrically active layer of strontium titanate with a figure of merit (curvature divided by electric field) of 3.33 MV^{-1}, comparable to that of state-of-the-art piezoelectric bimorph cantilevers.

Certain attributes of flexoelectricity point towards a favourable role in micro- and nano-electromechanical systems (MEMS and NEMS). First, flexoelectricity is a universal phenomenon exhibited by materials of all symmetry groups and thus flexoelectric devices can in principle be fabricated from silicon or any of its gate dielectrics in a completely complementary metal oxide semiconductor (CMOS)-compatible environment. Second, any (strain) gradient scales inversely with the material dimension[3], thus allowing flexoelectricity to match or even dominate over piezoelectricity at the nanoscale[4], particularly in materials with high dielectric permittivity ε, such as ferroelectric thin films[5] and composites[6]. Third, high-frequency bending resonators capable of functioning at extreme temperatures can be implemented. Fourth, flexoelectric devices can be made from simple dielectrics, with a performance that is therefore linear and non-hysteretic. Finally, a flexoelectric, unlike a piezoelectric bimorph actuator, does not need to be clamped to an elastic passive layer in order to bend: a single dielectric layer is sufficient to achieve field-induced bending, and this simplifies device design and removes the risk of delamination that can exist at the clamping interface of standard piezoelectric bimorph actuators (Fig. 1).

In contrast, because the materials with the largest piezoelectric coefficients are ferroelectric, piezo-electric devices can suffer from their intrinsically hysteretic nature and nonlinear behaviour at fields close to the coercive voltage, and their properties are also strongly temperature-dependent: they only work below their Curie temperature. Moreover, the ferroelectrics with the largest piezoelectric coefficients are lead-based[7], and lead toxicity poses serious problems for the integration of such devices in biomedical applications, where MEMS-based energy-harvesting devices would otherwise find a natural niche of applications[8]. In addition, bimorphs can also be restricted by the mechanical and thermal expansion mismatch between the piezoelectric and elastic layers, which can lead to progressive deterioration of the bonding between the layers.

Despite the advantages offered by nanoscale flexoelectricity, research in this field is still in its infancy[9,10], and considerable effort is required before it can be established as a viable technology. On the fundamental front, we need a reliable catalogue of flexoelectric coefficients for all materials of technological interest, as well as proof that the magnitude of these coefficients remains constant at the nanoscale. On the practical front, we need to develop both nanofabrication and nano-characterization tools suitable for making and measuring flexoelectric nanodevices. This article addresses these two issues.

We fabricated all-oxide nanocantilevers (Fig. 2a) as capacitor structures composed of a strontium titanate ($SrTiO_3$) active layer sandwiched between two layers of strontium ruthenate ($SrRuO_3$)

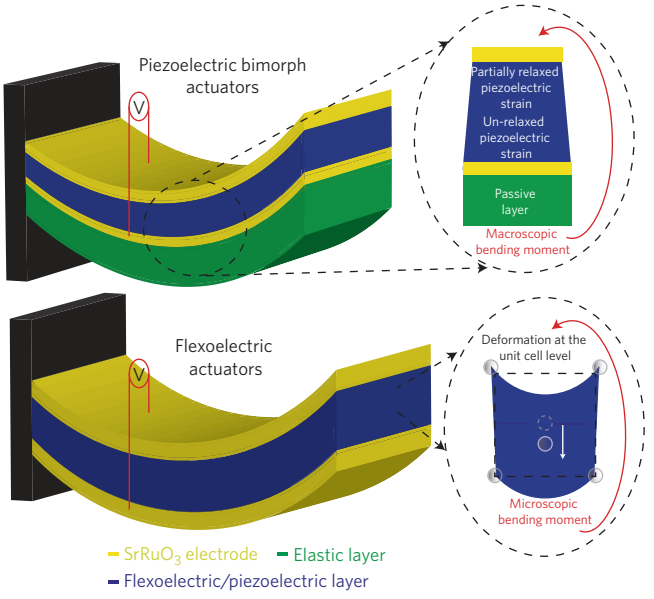

Figure 1 | Schematic comparing flexoelectric actuation and piezoelectric bimorph actuation in nanoscale actuators. In a piezoelectric bimorph actuator, a homogeneous mechanical strain is generated on application of an electrical voltage to the piezoelectric layer. The mechanical clamping induced by the non-piezoelectric layer creates a strain gradient across the structure, converting the piezoelectric strain into a flexural motion. On the other hand, any dielectric sandwiched between the electrodes can, in principle, act as a flexoelectric actuator. In this case, the bending moment arises from a symmetry-breaking strain gradient generated at the unit cell level.

[1]ICN2 – Institut Catala de Nanociencia i Nanotecnologia, CSIC and The Barcelona Institute of Science and Technology, Campus UAB, Bellaterra, Barcelona 08193, Spain. [2]Faculty of Science and Technology and MESA+ Institute for Nanotechnology, University of Twente, PO Box 217, AE Enschede 7500, The Netherlands. [3]Department of Materials Science and Engineering, Cornell University, Ithaca, New York 14853, USA. [4]Kavli Institute at Cornell for Nanoscale Science, Ithaca, New York 14853, USA. [5]ICREA – Institucio Catalana de Recerca i Estudis Avançats, Barcelona 08010, Spain. †These authors contributed equally to this work. *e-mail: umeshkbhaskar@icn.cat; gustau.catalan@icn.cat

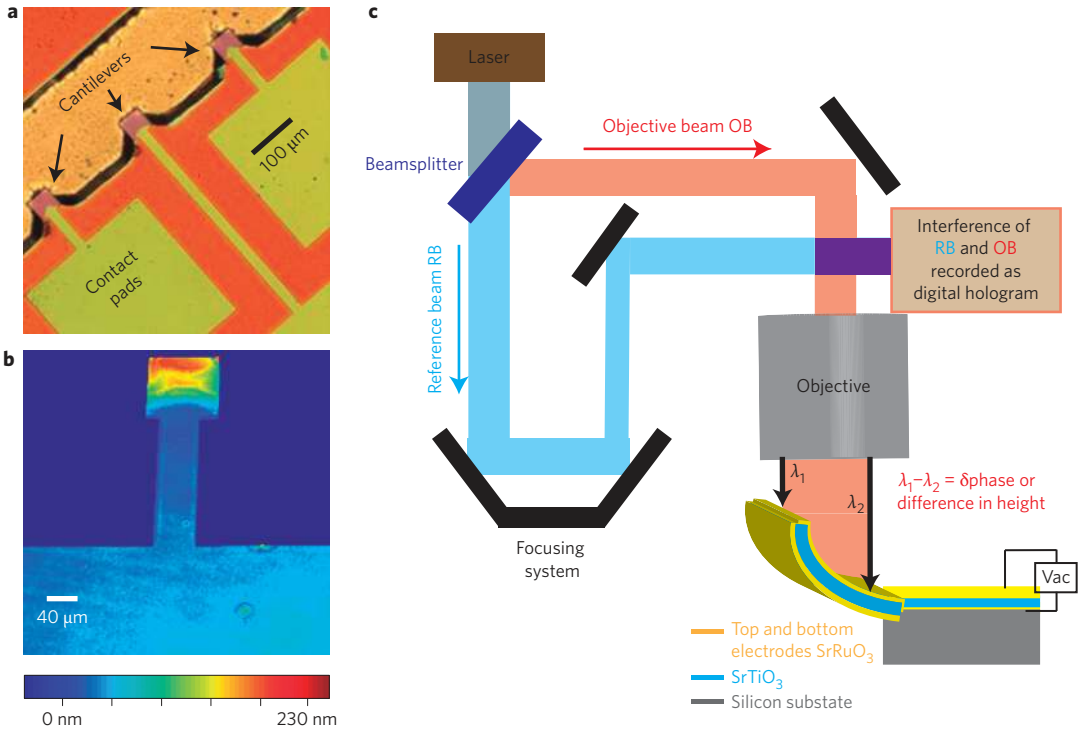

Figure 2 | Experimental design. a, Optical image of an array of $SrTiO_3$ nanocantilevers. **b**, Three-dimensional image of one $SrTiO_3$ nanocantilever with colour scale corresponding to the out-of-plane displacement. **c**, The digital holographic microscope splits a coherent laser beam into an objective beam and a reference beam. The objective beam is focused onto the sample and the light reflected is collected to form an interference pattern with the reference beam. Any difference in height along the sample surface results in a corresponding difference in the phase of the light reflected back from it.

for the top and bottom electrodes. The complete capacitor stack (Supplementary Figs 1 and 2) was grown epitaxially on a buffer of $SrTiO_3$ deposited by molecular beam epitaxy (MBE) on silicon, which is currently an established template system for incorporating other epitaxial oxide films on silicon[6]. Details of the fabrication are provided in the Methods. The centrosymmetric lattice of room-temperature $SrTiO_3$ ensures that any measured bending moment arises purely from flexoelecticity, and room-temperature paraelectricity in $SrTiO_3$ is also confirmed by its linear and non-hysteretic mechanical response as a function of electric field. For comparison, Supplementary Fig. 3 shows the characteristic butterfly-shaped hysteresis loop response of a ferroelectric lead zirconium titanate (PZT) cantilever grown by similar methods on silicon. $SrTiO_3$ is also currently the only (bulk) material for which the theoretical and experimental values (measured using the direct method) are of the same order of magnitude[11], providing a good reference for testing two important questions: (1) whether the bulk flexoelectric coefficients retain their bulk value in thin films and (2) whether the coefficients measured by us using the inverse method (actuator mode) are the same as those measured in bulk by the direct method (sensor mode), something that is definitely true for piezoelectrics but is not obvious in flexoelectricity, where this question has been controversial[12].

The most popular method currently used to characterize flexoelectric coefficients involves dynamically bending a cantilever and using lock-in techniques to instantaneously measure the charge generated by the bending. We refer to this as the direct method, and it has been applied to a variety of materials, including perovskite ceramics[13], single crystals[11] and even polymers[17]. Its drawback is the difficulty of miniaturizing mechanical bending appliances down to the nanoscale. However, while direct flexoelectricity measures the polarization induced by bending, a converse or inverse effect also exists whereby polarizing a sample causes it to bend[2,12,14–16]. The 'inverse method' thus involves the application of an electric field to a cantilever or plate-shaped material, and measuring the induced bending[14,15]. The curvature k induced via flexoelectricity μ is related to the flexural rigidity D of the plate and the applied voltage V by[9]

$$k = \frac{\mu V}{D} \quad (1)$$

The flexural rigidity D of a cantilever is given by $(Et^3)/(12(1-\nu^2))$, where E is Young's modulus, ν is the Poisson ratio, and t is the thickness. The flexoelectrically induced curvature k thus scales as the cube of the cantilever thickness; that is, the voltage-induced bending multiplies by a factor of 8, almost an order of magnitude, every time the thickness is halved. The inverse scaling of k with Young's modulus also makes it pertinent for the characterization of soft materials, which are expected to display giant electromechanical coupling[18]. On the practical side, achieving converse flexoelectricity only requires the fabrication of planar capacitive cantilevers, and we demonstrate that this requirement can be readily realized using existing MEMS techniques. Thus, inverse flexoelectricity is an optimum route to explore and exploit the flexoelectricity of nanodevices.

The observation of cantilever oscillations induced by an applied alternating voltage (V_{ac}) was made using a commercial digital holographic microscope[19,20] (DHM; schematically illustrated in Fig. 2b,c) working in stroboscopic mode. The Fourier-filtered first-harmonic displacement induced in the $16 \times 40\ \mu m^2$ $SrTiO_3$ cantilever plate is plotted as a function of a.c. excitation at 100 kHz and just above resonance (320 kHz) in Fig. 3a,b respectively (the unfiltered response at 100 kHz is shown in Supplementary Fig. 4). The curvature was calculated from the Fourier-filtered displacement[21]. To probe the dynamics further, the cantilever was excited with the same bias of 1 V but over a range of different sinusoidal frequencies (Fig. 3c). The observed resonance frequency of ~310 kHz corresponds quite well with the analytical estimate based on the geometry

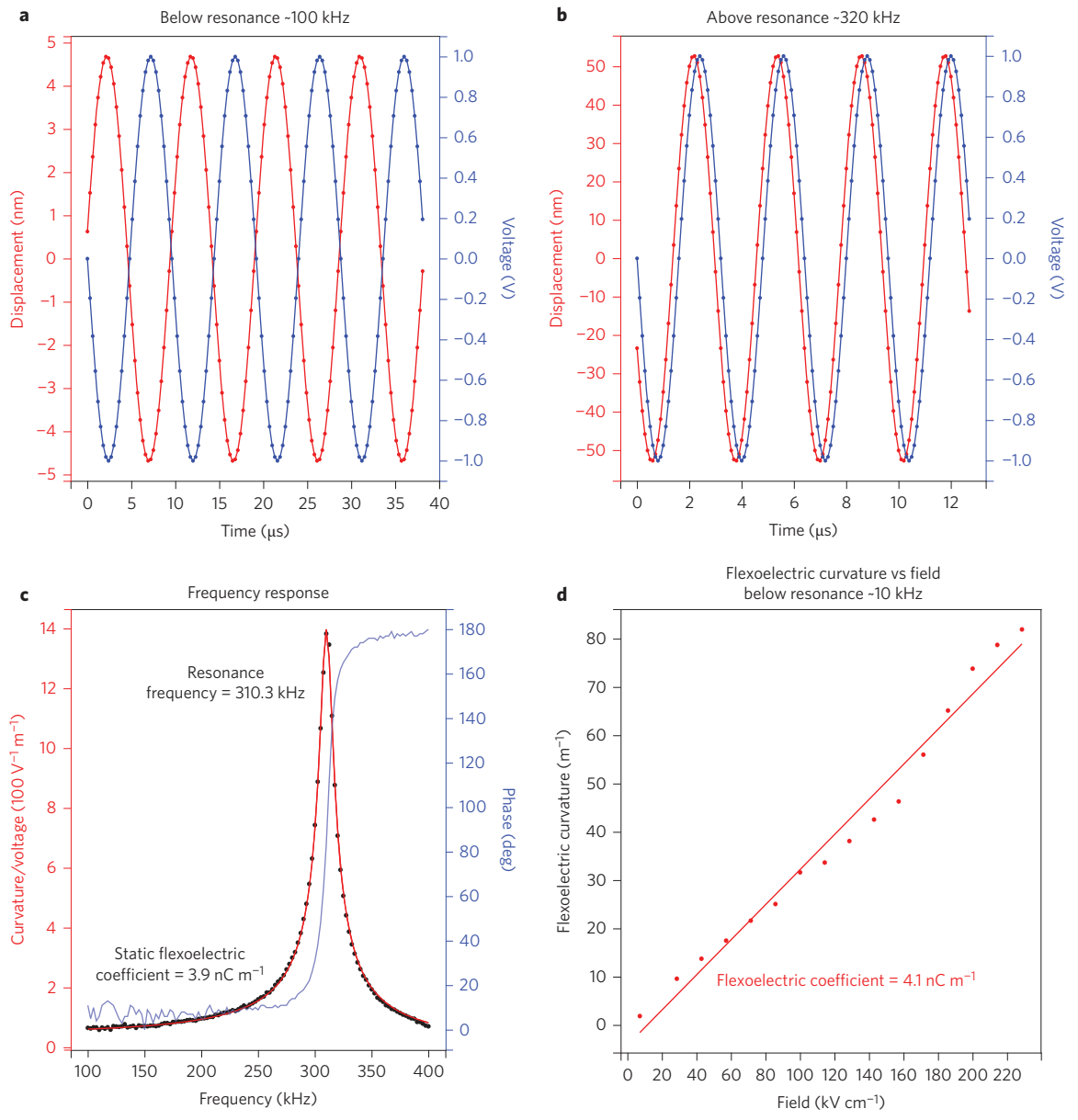

Figure 3 | Experimental characterization of flexoelectricity as a function of frequency and electric field. a,**b**, A.c. voltage and first-harmonic displacement, for an applied voltage of 1 V, plotted for the cantilever below (**a**) and above (**b**) the resonance frequency. **c**, Curvature/voltage ratio as a function of frequency for the $SrTiO_3$ nanocantilever at 1 V excitation, showing the resonant peak at ~310 kHz. The quality factor Q is ~25. The resonance is confirmed by the 180° phase change. **d**, The first-harmonic flexoelectric curvature shows a linear variance when plotted as a function of the applied a.c. field. The frequency of the measurement was 100 kHz, well below the resonant frequency amplification and close to the intrinsic static performance calculated from the fit in **c**.

of the cantilever (Supplementary Fig. 5), while the phase corresponds to the lag between the waveform of the excitation signal (voltage) and that of the flexoelectric response (deflection).

The first-harmonic curvature measured as a function of applied a.c. field at ~100 kHz is plotted in Fig. 3d and shows the expected linear behaviour for a flexoelectric actuator. To demonstrate the stability of the measurements (that is, away from resonance and close to the static limit) as a function of frequency, a complete curvature versus field measurement made at 10 kHz is presented in Supplementary Fig. 6. The value of the flexoelectric coefficient μ_{eff} calculated from the slope of the curvature versus voltage using equation (1) yields $\mu_{\mathrm{eff}} \approx 4.6$ nC m^{-1}. This is an effective flexoelectric coefficient that involves a geometry-dependent combination of the flexoelectric tensor components. Calculations using a self-consistent continuum model of flexoelectricity[15], under the assumption that the ratio between μ_{11} and μ_{12} remains the same as in bulk[11], yield $\mu_{12} \approx 4.1$ nC m^{-1}. (μ_{11} and μ_{12} are the longitudinal and transverse components of the cubic flexoelectric tensor, respectively.) This is comparable to the μ_{12} for bulk $SrTiO_3$ (100) crystals measured by the direct method ($\mu_{12} \approx 7$ nC m^{-1})[11], particularly when factoring in the smaller relative permittivity of our $SrTiO_3$ thin film, which is approximately four times smaller than that of bulk single crystals. Indeed, the quantity of physical significance[9] is the flexocoupling ratio $f = \mu/\varepsilon$, which is 6 V for our $SrTiO_3$ nanocantilevers, in good agreement with the estimate proposed by Kogan of 1–10 V for ionic solids[1] and comparable to the value found for other perovskites such as lead magnesium niobate–lead titanate (PMN-PT)[22]. The similarity of the coefficients measured by inverse and direct methods also provides experimental validation that flexoelectric devices will display the same coupling constant for operation as a sensor and actuator[12].

Figure 4 compares the actuation performance of our flexoelectric cantilever and that of state-of-the-art piezoelectric bimorph

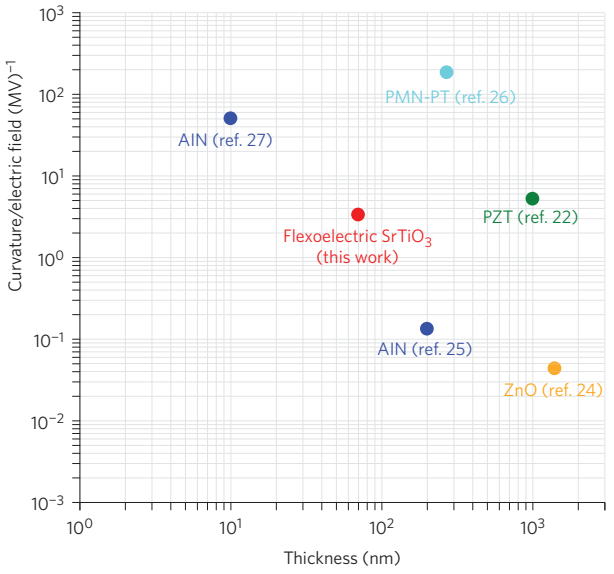

Figure 4 | Comparison of the performance of flexoelectric $SrTiO_3$ with those of state-of-the-art piezoelectric bimorphs. The ratios of the curvature/electric field are compared for flexoelectric $SrTiO_3$ and piezoelectric devices fabricated from ZnO[23], AlN[24,26], PZT[21] and PMN-PT[25]. For all materials, the plotted value corresponds to the intrinsic response measured out of resonance.

cantilevers fabricated using ZnO[23], AlN[24], PZT[21] and PMN-PT[25]. The electromechanical performance (the curvature/electric field ratio) of our $SrTiO_3$ devices (3.33 MV^{-1}) is comparable to or larger than those of devices fabricated using ZnO[23] (0.044 MV^{-1}), AlN[24] (0.133 MV^{-1}) and PZT[21] (5.208 MV^{-1}), and lower than that of hyper-active PMN-PT[25] (184.4 MV^{-1}) and an optimal ultrathin device made with a 10-nm-thick AlN[26] (50.3 MV^{-1}) active layer. However, the flexoelectric curvature/voltage scales as the inverse of the cube of the thickness (equation (1)), so $SrTiO_3$ devices with the same thickness as the state-of-the-art AlN[26] could be expected to exceed the performance of even the best piezoelectric and ferroelectric devices reported in the literature to date. We have also programmed an open-access App (https://umeshkbhaskar.shinyapps.io/FlexovsPiezo_app) to facilitate a direct comparison of the expected performances of piezoelectric and flexoelectric actuators for different cantilever geometries and material specifications.

In conclusion, we have shown that flexoelectricity can be exploited to fabricate lead-free electromechanical actuators that can be integrated on silicon for MEMS and NEMS applications. Looking beyond $SrTiO_3$, all high-k dielectric materials used in CMOS circuitry should in principle also be flexoelectric, because this is a property that is not restricted by material symmetry[9]. An extensive catalogue of materials is thus likely to be suitable for nanoscale electromechanical device applications, providing a route to integrating 'more than Moore' electromechanical functionalities within transistor technology.

Methods

Methods and any associated references are available in the online version of the paper.

Received 20 March 2015; accepted 7 October 2015; published online 16 November 2015

References

1. Kogan, S. Piezoelectric effect during inhomogeneous deformation and acoustic scattering of carriers in crystals. *Sov. Phys. Solid State* **5,** 2069–2079 (1964).
2. Bursian, E. & Trunov, N. Nonlocal piezoelectric effect. *Sov. Phys. Solid State* **16,** 760–762 (1974).
3. Gregg, J. M. Stressing ferroelectrics. *Science* **336,** 41–42 (2012).
4. Majdoub, M., Sharma, P. & Çağin, T. Dramatic enhancement in energy harvesting for a narrow range of dimensions in piezoelectric nanostructures. *Phys. Rev. B* **78,** 121407 (2008).
5. Lee, D. *et al.* Giant flexoelectric effect in ferroelectric epitaxial thin films. *Phys. Rev. Lett.* **107,** 057602 (2011).
6. Cross, L. Flexoelectric effects: charge separation in insulating solids subjected to elastic strain gradients. *J. Mater. Sci.* **41,** 53–63 (2006).
7. Cross, E. Lead-free at last. *Nature* **32,** 24–25 (2004).
8. Dreyfus, R. *et al.* Microscopic artificial swimmers. *Nature* **437,** 862–865 (2005).
9. Zubko, P., Catalan, G. & Tagantsev, A. K. Flexoelectric effect in solids. *Annu. Rev. Mater. Res.* **43,** 387–421 (2013).
10. Biancoli, A., Fancher, C. M., Jones, J. L. & Damjanovic, D. Breaking of macroscopic centric symmetry in paraelectric phases of ferroelectric materials and implications for flexoelectricity. *Nature Mater.* **14,** 224–229 (2014).
11. Zubko, P., Catalan, G., Buckley, A., Welche, P. & Scott, J. Strain-gradient-induced polarization in $SrTiO_3$ single crystals. *Phys. Rev. Lett.* **99,** 167601 (2007).
12. Breger, L., Furukawa, T. & Fukada, E. Bending piezoelectricity in polyvinylidene fluoride. *Jpn J. Appl. Phys.* **15,** 2239–2240 (1976).
13. Tagantsev, A. K. & Yurkov, A. S. Flexoelectric effect in finite samples. *J. Appl. Phys.* **112,** 044103 (2012).
14. Bursian, E. & Zaikovskii, O. I. Changes in curvature of ferroelectric film due to polarization. *Sov. Phys. Solid State* **10,** 1121–1124 (1968).
15. Abdollahi, A., Peco, C., Millán, D., Arroyo, M. & Arias, I. Computational evaluation of the flexoelectric effect in dielectric solids. *J. Appl. Phys.* **116,** 093502 (2014).
16. Zalesskii, V. G. & Rumyantseva, E. D. Converse flexoelectric effect in the $SrTiO_3$ single crystal. *Phys. Solid State* **56,** 1352–1354 (2014).
17. Deng, Q., Liu, L. & Sharma, P. Electrets in soft materials: nonlinearity, size effects, and giant electromechanical coupling. *Phys. Rev. E* **90,** 012603 (2014).
18. Baek, S.-H. & Eom, C.-B. Epitaxial integration of perovskite-based multifunctional oxides on silicon. *Acta Mater.* **61,** 2734–2750 (2013).
19. Cotte, Y., Toy, F., Jourdain, P. & Pavillon, N. Marker-free phase nanoscopy. *Nature Photon.* **7,** 113–117 (2013).
20. Colomb, T., Krivec, S. & Hutter, H. Digital holographic reflectometry. *Opt. Express* **21,** 12643–12650 (2013).
21. Dekkers, M. *et al.* The significance of the piezoelectric coefficient $d_{31,eff}$ determined from cantilever structures. *J. Micromech. Microeng.* **23,** 025008 (2013).
22. Narvaez, J. & Catalan, G. Origin of the enhanced flexoelectricity of relaxor ferroelectrics. *Appl. Phys. Lett.* **104,** 162903 (2014).
23. Wang, P., Du, H., Shen, S., Zhang, M. & Liu, B. Preparation and characterization of ZnO microcantilever for nanoactuation. *Nanoscale Res. Lett.* **7,** 176 (2012).
24. Doll, J. C., Petzold, B. C., Ninan, B., Mullapudi, R. & Pruitt, B. L. Aluminum nitride on titanium for CMOS compatible piezoelectric transducers. *J. Micromech. Microeng.* **20,** 025008 (2009).
25. Baek, S. H. *et al.* Giant piezoelectricity on Si for hyperactive MEMS. *Science* **334,** 958–961 (2011).
26. Zaghloul, U. & Piazza, G. 10–25 NM piezoelectric nano-actuators and NEMS switches for millivolt computational logic. *Proc. IEEE Int. Conf. Micro Electro Mech. Syst.* 233–236 http://dx.doi.org/10.1109/MEMSYS.2013.6474220 (2013).

Acknowledgements

The work at ICN2 was funded by an ERC Starting Grant from the EU (Project No. 308023), a National Plan grant from Spain (FIS2013-48668-C2-1-P) and the Severo Ochoa Excellence programme. The work at Cornell University was supported by the National Science Foundation (Nanosystems Engineering Research Center for Translational Applications of Nanoscale Multiferroic Systems) under grant number EEC-1160504. The authors thank E. Cuche, J. Parent, E. Solanas and Y. Emery for discussions.

Author contributions

G.C. and U.B. conceived and designed the experiments. N.B. designed and made the cantilevers under the supervision of G.R. U.B. performed and analysed the inverse flexoelectric characterizations under the supervision of G.C. A.A. performed the self-consistent continuum modelling and simulations. Z.W. performed the molecular beam epitaxy growth of the template layer under the supervision of D.S. U.B. and G.C. wrote the paper with the help of all the other authors. All authors discussed the results, commented on the manuscript and gave their approval to the final version of the manuscript.

Additional information

Supplementary information is available in the online version of the paper. Reprints and permissions information is available online at www.nature.com/reprints. Correspondence and requests for materials should be addressed to U.K.B. and G.C.

Competing financial interests

The authors declare no competing financial interests.

Methods

Fabrication of nanocantilevers. All-oxide epitaxial flexoelectric MEMS devices were grown by pulsed laser deposition patterned using a liftoff[27] method, and finally released via anisotropic substrate etching (Supplementary Fig. 1). To ensure the (001) epitaxial growth of the perovskites on silicon, an epitaxial $SrTiO_3$ buffer layer (~30 nm) was grown by MBE[28]. The functional $SrTiO_3$ layer (~70 nm), and the $SrRuO_3$ (~25 nm) electrode layers surrounding it, were grown epitaxially (Supplementary Fig. 2) using pulsed laser deposition. A sacrificial mask-assisted liftoff technique was used to pattern the heterostructures in a single liftoff step[27]. The top $SrRuO_3$ electrode layer was patterned using ion-beam etching. After patterning the perovskite layers, the free-standing devices were released by anisotropic KOH etching of the silicon substrate. Owing to the different numbers of exposed dangling bonds in the different crystal planes of silicon, there is strong anisotropy in the etching rate. Hence, control of the cantilever in-plane orientation with respect to the substrate crystal axis is crucial for achieving the desired release rate and minimizing any etching-related damage[29]. The released length of the cantilever plate was 16 μm.

Detection of cantilever vibrations using the DHM. The DHM synchronizes the image acquisition frequency with the frequency of sinusoidal excitation applied to the cantilever to ensure that the periodic movement of the cantilever is completely captured as a sequential array of static holograms. Each hologram captured by the DHM (Fig. 2c) is simultaneously resolved into an intensity image, which is similar to a single-wavelength microscope image, and a phase image, which maps the topographic profile of the sample. The phase images calculate the topography based on the path difference of light reflected by the surface and a specified reference frame. By placing this reference on the base of the cantilever, each phase image provides the full profile—including the curvature—of the cantilever. By its nature, the measurement is insensitive to any voltage-induced homogenous expansions or deformations and only records voltage-induced changes in the slope and curvature of the cantilever. The periodic displacement in response to an applied a.c. excitation was found to contain both first-harmonic (1ω) and second-harmonic contributions (2ω). To obtain the strength of purely the flexoelectric response (which is linearly proportional to the field and therefore a first-harmonic oscillation), Fourier filtering or harmonic regression was used to quantify the 1ω bending.

Self-consistent continuum model of flexoelectricity. By using a self-consistent continuum model of flexoelectricity[15], we performed simulations of the multilayer cantilever beam under the application of an electric field. The aspect ratio of the beam was fixed to $L/h = 10$, where L and h are the length and height of the beam. A larger aspect ratio leads to almost identical results. The electric potential was fixed to zero on the top electrode, and we constrained the electric potential on the bottom electrode to a constant value, generating the same magnitude of applied electric field as in the experiments. The material parameters were chosen according to the composition of the multilayer cantilever. We consider $\mu_{12} = -10\mu_{11}$, as reported from a direct measurement on $SrTiO_3$ (ref. 11). Simulation results show that the cantilever is deflected under the applied electrical load, supporting the experimental observations that a cantilever beam can deform, as an electromechanical actuator, due to flexoelectricity.

References

27. Banerjee, N., Koster, G. & Rijnders, G. Submicron patterning of epitaxial $PbZr_{0.52}Ti_{0.48}O_3$ heterostructures. *Appl. Phys. Lett.* **102,** 142909 (2013).
28. Warusawithana, M. P. *et al.* A ferroelectric oxide made directly on silicon. *Science* **324,** 367–370 (2009).
29. Banerjee, N., Houwman, E. P., Koster, G. & Rijnders, G. Fabrication of piezodriven, free-standing, all-oxide heteroepitaxial cantilevers on silicon. *APL Mater.* **2,** 096103 (2014).